EVALUATING CRUSTAL CONTAMINATION EFFECTS ON THE LITHOPHILE TRACE ELEMENT BUDGET OF SHERGOTTITES, NWA 856 AS A TEST CASE. A. D. Brandon[1], J. Ferdous[1], and A. H. Peslier[2], [1]Department of Earth and Atmospheric Sciences, University of Houston, Houston, TX 77204, abrandon@uh.edu , [2]Jacobs, NASA-Johnson Space Center, Mail Code X13, Houston TX 77058.

Introduction: The issue of whether crustal contamination has affected the lithophile trace element budget of shergottites has been a point of contention for decades [1-7]. The evaluation has focused on the enriched shergottite compositions as an outcome of crustal contamination of mantle-derived parent magmas or, alternatively, the compositions of these stones reflect an incompatible trace element (ITE) enriched mantle source.

Recent findings have supported the notion that enriched shergottite compositions reflect crustal contamination. For example, ITE-enriched olivine-hosted melt inclusions have been found in depleted shergottites [7], the rare earth element (REE) compositions of Mars crustal sample NWA 7034 and its paired stones, when mixed with depleted shergottite compositions, adequately reproduce the bulk REE compositions of enriched shergottites [8,9]. These two results are consistent with findings from Cl and S isotopes that indicate shergottite magmas interact with martian crust on their way to or, on the surface [10,11]. However, a crustal contamination model must adequately explain not only the ITE compositions of enriched shergottites, but also their lithophile element isotope compositions such as for Nd and Sr isotopes. Using Os-Nd isotope relationships, realistic crustal contamination models have been shown to not work to produce enriched shergottites from depleted shergottite parent magmas [12,13]. Hence the origin of the ITE-enrichment in enriched shergottites remains an open question.

To further evaluate this issue, a comprehensive study on enriched shergottite NWA 856 [14] was undertaken, building on a previous ^{87}Rb-^{87}Sr and ^{147}Sm-^{143}Nd isotope chronology study [15]. The new work included major and trace element analyses of minerals, and evaluated the crystallization history of NWA 856. This stone has a bulk molar Mg# of 0.49 and lacks olivine, making it one of the most evolved members of the enriched shergottites. Hence, this stone underwent extensive crystallization from its parent magma such that there was a strong prospect for crustal contamination during its evolution. In addition, Nd isotope compositions have recently been reported for Mars crustal breccia NWA 7034 [8,16]. Combining these new data with the comprehensive data available for shergottites allow for a refined evaluation of the effects of crustal contamination and its implications to shergottite source variation in the martian mantle and crust.

Results: The previously reported ^{87}Rb-^{87}Sr and ^{147}Sm-^{143}Nd results were re-evaluated for ages using ISOPLOT. The new computations give ^{87}Rb-^{87}Sr and ^{147}Sm-^{143}Nd internal isochron ages of 162±14 Ma (±2σ and used herein) and 162.7±5.5 Ma, respectively, with an initial εNd = -6.6±0.2. These ages fall in the range for those of the other enriched shergottites that when combined give an average Nd isotopic age of 173±22 Ma, equivalent to an average age of 175 Ma proposed by [6].

The bulk rock composition of NWA 856 was used in MELTS simulations to model equilibrium and fractional crystallization sequences to compare with the crystallization sequence from textural observations and to the mineral compositions. These models constrain the depth of initial crystallization to a pressure range of 0.4-0.5 GPa (equivalent to 34-42 km) in anhydrous conditions at the Fayalite-Magnetite-Quartz buffer, and consistently reproduce the observed mineralogy throughout the sequence with progressive crystallization. The REE abundances in the clinopyroxenes and maskelynite are consistent with progressive crystallization in a closed system. Closed system crystallization also explains best the compositions of other enriched shergottites including LAR 06319 [17] and NWA 5298 [18].

The Ti/Al ratios in the NWA 856 clinopyroxenes are consistent with initial crystallization occurring at the lower crust to uppermost mantle depths constrained by the MELTS models followed by polybaric crystallization as the parent magma ascended to the surface. Polybaric crystallization is recorded in pyroxene Ti/Al ratios for a wide range of depleted and enriched shergottites including for example, depleted shergottite NWA 5789 [19], and enriched shergottites RBT 04262, NWA 5398, LAR 06319, Zagami, Los Angeles, and Shergotty (not shown).

Discussion: The mechanisms of crustal contamination in terrestrial mafic magmas are well understood [20-22]. Crystallization provides latent heat that can then be used to melt the surrounding crust. Two end-member scenarios of crustal contamination are possible, one where the compositional outcomes will follow trends of assimilation and contemporaneous fractional crystallization (AFC), or they will simply follow mixing trends between compositional end-members. Any successful model that ascribes compositional variabil-

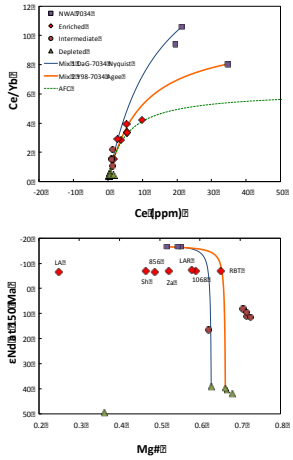

Figure 1. AFC and mixing of crust with depleted shergottite models. Bulk rock

ity to any given related suite of mafic srocks to crustal contamination should thus be able to predict the outcomes for major element, trace element, and isotopic variability. As noted above, the bulk and mineral compositions of depleted and enriched shergottites, including NWA 856, indicate that polybaric crystallization occurred while shergottite parent magmas were transported through the martian crust and underwent variable amounts of differentiation. Hence there was ample opportunity for shergottite magmas to interact with the martian crust and inherit its compositional signatures either through AFC processes or mixing between shergottite parent magmas and crust.

The trends for mixing between depleted shergotite compositions with martian crust represented by NWA 7034 are compared to the compositional variation displayed by all shergottites (Figure 1). For Ce versus Ce/Yb, both mixing and AFC models can explain the bulk rock variation observed in intermediate and enriched shergottites as interaction of depleted shergottite magmas with martian crust. This is consistent with previous proposals that their REE budgets resulted from crustal contamination [8,9]. The crust-depleted shergottite mixing and AFC models plot through the high molar Mg#-εNd data for enriched shergottites such as those for RBT 04262. However, the models fail to produce, for example, the restricted range of εNd at 150 Ma of -6.8±0.6 over a wide range of molar Mg# from 0.65 to 0.25 (Figure 1), or the range of Ce/Yb ratios versus molar Mg# (not shown). As the amount of crust proportions increases during progressive mixing or AFC in a differentiating shergottite magma, all of the models predict that the respective molar Mg# decreases, and that εNd would instead show a progressive decrease in the evolved magmas. Hence, the constant εNd of enriched shergottites over a wide range of differentiation indices is not an outcome of crustal contamination of a depleted shergottite parent magma.

The only crustal contamination model that can explain the bulk lithophile ITE compositions of enriched shergottites is one where primitive, high molar Mg# magmas experience crustal contamination, that is then subsequently shut down or strongly minimized during the remaining differentiation. While not impossible, evidence from terrestrial systems show instead that crustal contamination is a progressive process during differentiation of mafic magmas [20-22]. Hence, it is concluded here that the bulk lithophile ITE budget of enriched shergottites represents instead a mantle source characteristic, likely formed during the early differentiation history of Mars [4-6].

References: [1] Jones J.H. (1986) *GCA 50, 969.* [2] Jones J.H. (2015) *MAPS* doi: 10.1111/maps.-12421. [3] Nyqyist L.E. et al. (2001) *Space Sci. Rev.* 96, 105. [4] Borg LE. and Draper D.S. (2003) *MAPS*, 38, 1713.[5] Debaille V. et al. (2008) *EPSL* 269, 186. [6] Symes S.J.K. et al. (2008) *GCA* 72, 1696. [7] Peters T.J. et al. (2015) *EPSL* 418, 91. [8] Agee C.B. et al. (2013) *Science*, 339 780. [9] Humayun M. et al. (2013) *Nature* 503, 513. [10] Franz H.B. et al. (2014) *Nature* 508, 364. [11] Williams J.R. et al. (2016) *Maps*, doi: 10.1111/maps.12647. [12] Brandon A.D. et al. (2000) *GCA* 64,4083. [13] Brandon A.D. et al. (2012) *GCA* 76, 206. [14] Jambon A. et al. (2002) *MAPS* 37, 1147. [15] Brandon A.D. et al. (2004) *LPS XXXV*, #1931. [16] Nyquist L.E. et al. (2016) *MAPS* 51, 483. [17] Peslier A.H. et al. (2010) *GCA* 74, 4543. [18] Hui H. et al. (2011) *MAPS* 46, 1313. [19] Gross J. et al. (2011) *MAPS* 46, 116. [20] DePaolo D.J. (1981) *EPSL* 53, 189. [21] Brandon A.D. et al. (1993) *CMP* 114, 452. [22] McLeod et al. (2012), *Geology* 40, 435.